PDT-induced changes in light scattering from cells using lysosomal- vs. mitochondrial-localizing photosensitizers

Jeremy D. Wilson[a] and Thomas H. Foster[a,b]

[a]Department of Physics and Astronomy, University of Rochester, Rochester, NY 14627
[b]Department of Imaging Sciences, University of Rochester, Rochester, NY 14642

ABSTRACT

We have previously described changes in angle-resolved light scattering measured from intact cells in suspension subjected to photodynamic therapy using photosensitizers that localize primarily to mitochondria. These changes were analyzed with a Mie theory-based model. For the sensitizers Pc 4 and ALA-induced protoporphyrin IX, the scattering data from PDT-treated cells was consistent with a coated sphere model, in which mitochondrial morphology changes were the predominant mechanism governing the scattering changes. This interpretation was supported by electron microscopy. Here we describe quite different changes in angle-resolved light scattering from cells sensitized with the lysosomal-localizing photosensitizer LS11. Unlike the case of the mitochondrial-localizing photosensitizers, analysis of these post-treatment scattering data reveals a shift toward a larger mean organelle diameter in the larger of the two particle size distributions identified from Mie-theory analysis of scattering from control cells. Further, the post-treatment scattering angular distributions are well interpreted in terms of homogeneous rather than coated spheres. On the basis of these results and results of fluorescence microscopy of LS11-PDT treated monolayers, we propose that the initial, pre-treatment scatterer population is comprised of lysosomes and mitochondria. LS11 PDT ablates a significant fraction of the lysosomes, leaving a relatively unperturbed population of mitochondria to dominate the scattering. These findings suggest that scattering measurements are capable of reporting a variety of PDT-induced changes to cell organelles. They further suggest that photodynamic action is a useful biophysical tool for understanding basic mechanisms of light scattering from intact cells.

Keywords: Light scattering, Mie theory, lysosomes, photodynamic therapy

1. INTRODUCTION

The use of light scattering techniques to monitor changes in cells and in bulk tissue represents an interesting possible approach to noninvasive optical dosimetry in photodynamic therapy. PDT with certain photosensitizers induces early changes to mitochondrial morphology, which impose a specific signature in the angularly-resolved scattering measured from intact cells. In addition to its possible role as a reporter of PDT damage and biological response, light scattering from cells is interesting in its own right. Since the report by Perelman et al.[1] that singly-backscattered light was sensitive to nuclear morphology, the subject has attracted considerable attention in the biomedical optics literature. It has become important to understand more deeply the origins of the scattering centers in cells in order to interpret the signals that are measured in response to disease states and various perturbations. In this regard, PDT has a great deal to offer insofar as different photosensitizers sensitize different organelle populations. By perturbing different organelles and measuring the effects on the scattered light, it is possible to ascertain the extent to which specific organelles contribute to the total scattering signal. In these kinds of studies, we evaluate the potential for scattering to inform our understanding of PDT and also use PDT as a biophysical tool to study basic problems in light scattering from cells. Here we describe further the use of a Mie-theory based model in sizing the scattering centers in cells and report preliminary results from experiments in which a lysosome-localizing photosensitizer, LS11, is used to perturb the angularly resolved scattering measured from suspensions of tumor cells.

Optical Methods for Tumor Treatment and Detection: Mechanisms and Techniques in Photodynamic Therapy XV, edited by David Kessel, Proc. of SPIE Vol. 6139, 613903, (2006) · 1605-7422/06/$15 · doi: 10.1117/12.644907

2. METHODS

2.1 Angularly-resolved light scattering measurements

All angularly-resolved light scattering measurements were made using our home-built goniometer described previously[2]. Briefly, a scattering sample in aqueous suspension is placed in a cylindrical cuvette (Model 540.115, Helma, Plainview, NY), which is positioned above the center of a 30.5 cm diameter rotary stage (RT-12, Arrick Robotics, Tyler, TX). In a typical experiment, red light (632.8 nm) from a 20 mW helium-neon laser is directed through the cuvette. In all of our measurements, the laser is linearly polarized perpendicular to the surface of the rotary stage. Light scattered from the sample is passed through a pinhole mounted midway to the edge of the rotary stage and collected by an optical fiber (200 m core diameter, 0.22 NA) that is mounted at the edge. Light exiting the fiber is measured by a photodiode (Model 2001, New Focus, San Jose, CA) and digitized at 16 bits. A PC-controlled stepper motor rotates the stage continuously from approximately 5 – 110 degrees with respect to the forward direction of the laser at an angular resolution of 0.2 degrees. The angular position is read out from an optical encoder, and the stage position and photodiode voltage are simultaneously recorded. The data acquisition is automated and controlled by a home-built program written in LabView (National Instruments, Austin, TX). Each scan of the full angular range takes approximately 1 minute.

2.2 Fluorescence microscopy

EMT6 cells were grown on coverslips and incubated with an appropriate fluorescent dye. The images acquired using LysoTracker Blue and MitoTracker Green were imaged at 60x with a conventional inverted geometry Nikon Diaphot microscope using either a Hoechst (330-380 nm excitation, > 420 nm emission) or a GFP (460-490 nm emission, 510-540 nm emission) filter set and digitized at 16 bits with a Spot RT KE CCD (Diagnostic Instruments, Inc, Sterling Heights, MI). Images of LS11 fluorescence were acquired using our home-built laser scanning confocal microscope with a 639 nm excitation, a 660 nm dichroic, and a 645 nm long pass filter.

2.3 Electron microscopy

For electron microscopy, cells were grown on glass chamber slides and fixed in 0.1M phosphate-buffered 2.0% glutaraldehyde at room temperature for 2 hours. After repeated rinsing in 0.1 M phosphate buffer, the cells were post-fixed in 1.0% osmium tetroxide for 20 minutes. The slides were passed through a graded series of ethanol, infiltrated with Spurr epoxy resin, and fitted to inverted capsular molds containing fresh Spurr resin. After polymerization at 70° C, the hardened capsules containing the cells of interest were then "popped off" the surface of the glass slides by dipping the slides into liquid nitrogen. These blocks were trimmed and sectioned at 60-70 nm intervals with a diamond knife onto mesh copper grids. The grids were contrast-enhanced with uranyl acetate for 15 minutes and lead citrate for 10 minutes and examined and photographed for quantitative analysis with a Hitachi 7100 transmission electron microscope at magnifications ranging from 3000x to 30,000x.

3. RESULTS AND DISCUSSION

3.1 Surface area equivalent scattering from ellipsoidal mitochondria in the forward direction

In a previous study from our group, we reported that by analyzing angularly-resolved light scattering data within a Mie theory model by plotting the product of the scattering cross section, σ, and the particle density as a function of the particle diameter, we could robustly extract the sizes of the intracellular particles responsible for scattering light[3]. The study revealed that in our EMT6 cell line, as well as in AT3.1 cells measured by another laboratory[4], 2 m particles were the dominant light scatterers, with particle sizes ranging from about 1-4 m responsible for between 85-95% of the total scattered signal in the angular range 5-90 degrees.

Based on these sizes, as well as results of other studies[2], we have attributed the bulk of this signal to mitochondria, with the possibility of a contribution by lysosomes and the nucleus on the smaller and larger end of the particle size distribution, respectively. The ability to extract sizes of mitochondria, which are highly non-spherical objects, with a Mie theory model is quite reasonable in our geometry, as elongated particles scatter light like surface-area-equivalent

spheres for angles less than 90 degrees[5]. As verification that the mitochondria in our EMT6 cells are surface-area equivalents of the spherical particles extracted in our analysis of the scattering data, we examined transmission electron micrographs (TEM) as well as fluorescence images of mitochondria to obtain estimates of mitochondrial morphology and dimensions.

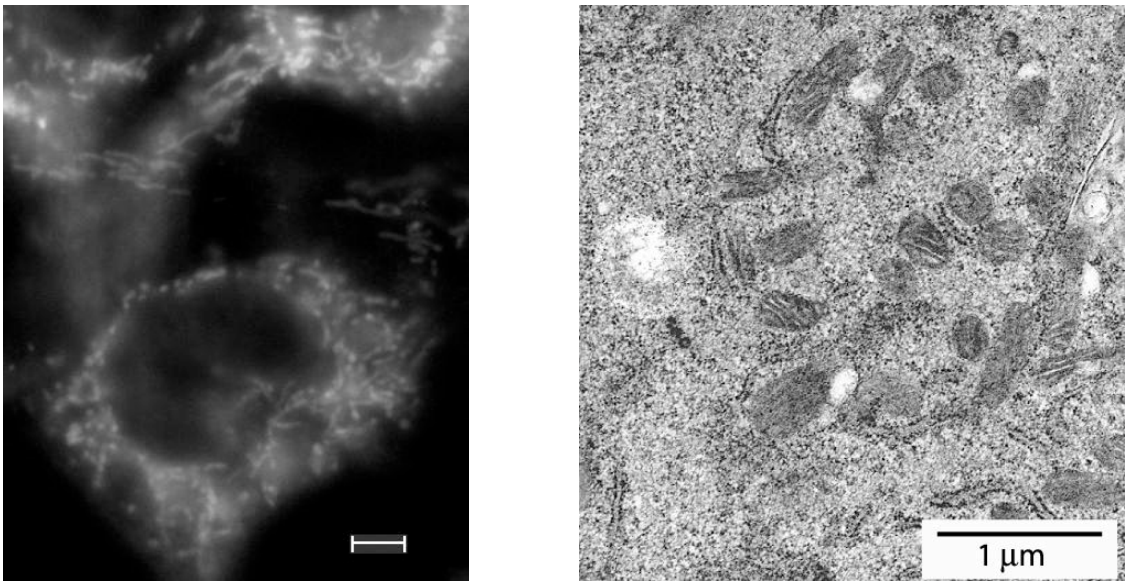

Figure 1. (Left) EMT6 cells stained with 100 nM MitoTracker Green and imaged under conventional fluorescence microscopy. Scale bar = 4 m. (Right) TEM micrograph of mitochondria from untreated EMT6 cells.

Figure 1 shows a fluorescence micrograph of EMT6 cells stained with 100 nM MitoTracker Green (Molecular Probes, Eugene, OR) and imaged with an appropriate filter set. The scale bar is 4 m, and it is clear that there are many mitochondria that are as long as or longer than the scale bar.

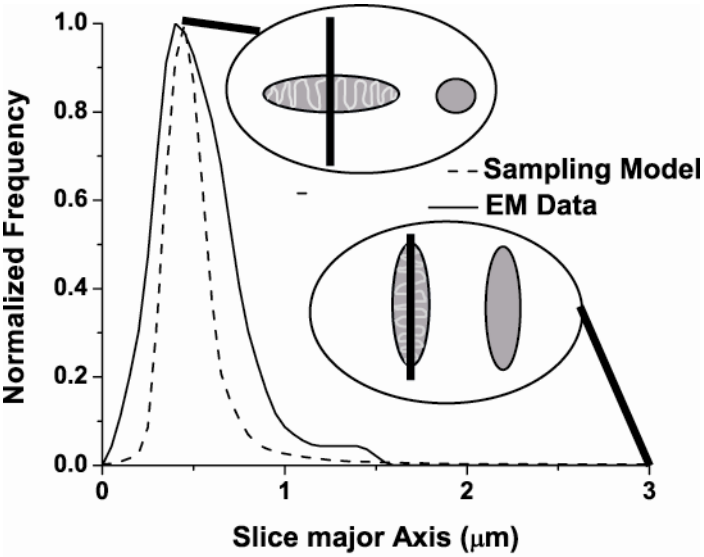

Figure 2. Frequency histograms of the major axis of ellipse slice for TEM images of mitochondria (solid line) and from a model of random sampling of a 0.5 x 4 m ellipse.

For the TEM images, the major axis of each ellipse slice was recorded for approximately 60 mitochondria, and histograms of this metric were built up. To interpret these histograms, we built a model in which an ellipse with major and minor axes of 4 and 0.5 m, respectively, was randomly sliced, thereby recreating the random sampling of ellipsoidal mitochondria in the thin TEM sections. The major axis of each of these slices was recorded, and similar histograms were created. A representative TEM micrograph is shown in Figure 1, and the analysis of the data and the sampling model are displayed in Figure 2.

From the TEM data as well as the fluorescence images, we can estimate that a typical EMT6 mitochondrion has a major and minor axis of 0.5 and 4 m, respectively, with mitochondria being as long as 4.5-5 m and as wide as 0.8 m. When the surface area of such an ellipsoid is taken into account, typical mitochondria should scatter like a 1.3 m-diameter sphere, with the outliers scattering like 2 and 3 m spheres. Figure 3 shows the primary particle size distribution extracted from Mie theory fits to angularly-resolved light scattering data from cells[3], and the above interpretation of mitochondrial sizes lends credence to interpreting the bulk of our scattering signal to mitochondria.

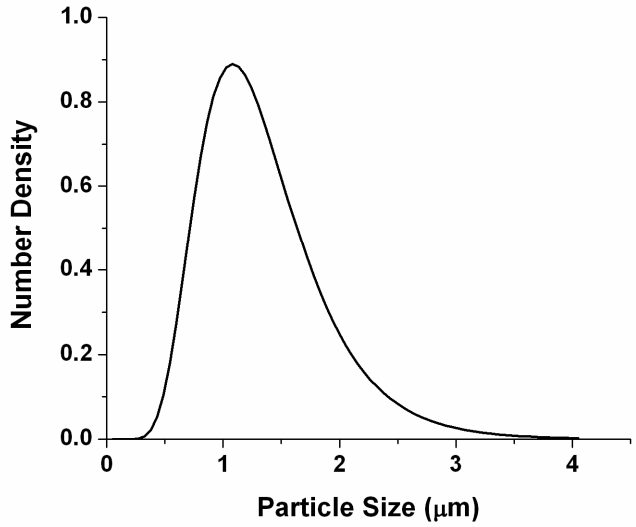

Figure 3. The larger of the two size distributions returned from Mie theory fits to angularly resolved light scattering data from intact EMT6 cells as reported in Wilson and Foster[3] with a mean of 1.1 m and a standard deviation of 0.6 m. As described in the text, this size distribution is consistent with scattering from ellipsoidal mitochondria with minor and major axes of 0.5 and 4.0 m, respectively.

3.2 Lysosomal scattering changes in LS11 PDT

The photosensitizer LS11 (N-aspartyl chlorin e6) is a proprietary photosensitzer of Light Sciences Corporation (Snoqualmie, WA). LS11 has been shown to localize to lysosomes, and at relatively low light doses induces apoptosis via the release of cytochrome c from the mitochondria[6]. Like other second generation photosensitizers, LS11 has a considerably higher extinction than drugs such as Photofrin® or ALA-induced PPIX. In this section, we take advantage of both the localization properties and high absorption cross section of LS11 to determine the lysosomal contribution to both the differential and total scattering cross sections of intact cells.

3.2.1 Scattering changes following ablation of lysosomes

We report here on the ability to detect differences in angularly-resolved light scattering between cells that were loaded with LS11 and subjected to high doses of PDT and cells that were not loaded with any drug. Preliminary microscopy experiments were preformed to obtain treatment conditions such that a significant fraction of lysosomes were ablated.

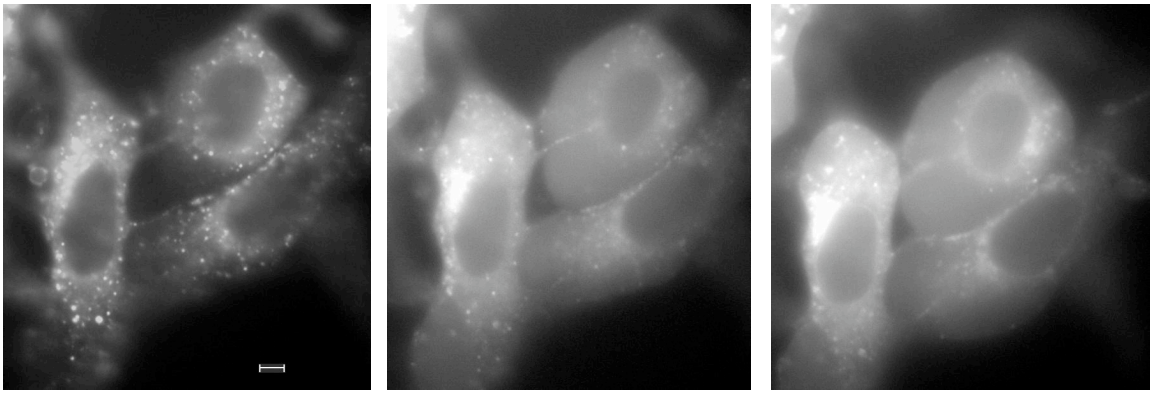

Figure 4. Cells loaded with both LS11 and LysoTracker blue and subjected to 0 (left), 10 (center), and 20 (right) J cm^{-2} at 662 nm. LysoTracker images were acquired with a Hoechst filter set.

Cells grown on coverslips were loaded with 50 g/mL LS11 in full serum media overnight and then co-stained with 75 nM LysoTracker blue (Molecular Probes, Eugene, OR). The cells were washed with Hanks' Balanced Salt Solution (HBSS) and imaged with a Hoechst filter set. Various light doses were given between 100 mJ cm^{-2} - 30 J cm^{-2} of total fluence from a 662 nm diode laser. The progression from 0-20 J cm^{-2} is displayed in Figure 4. From these data, we found that we needed between 10 and 20 J cm^{-2} to obliterate a significant fraction of the lysosomes.

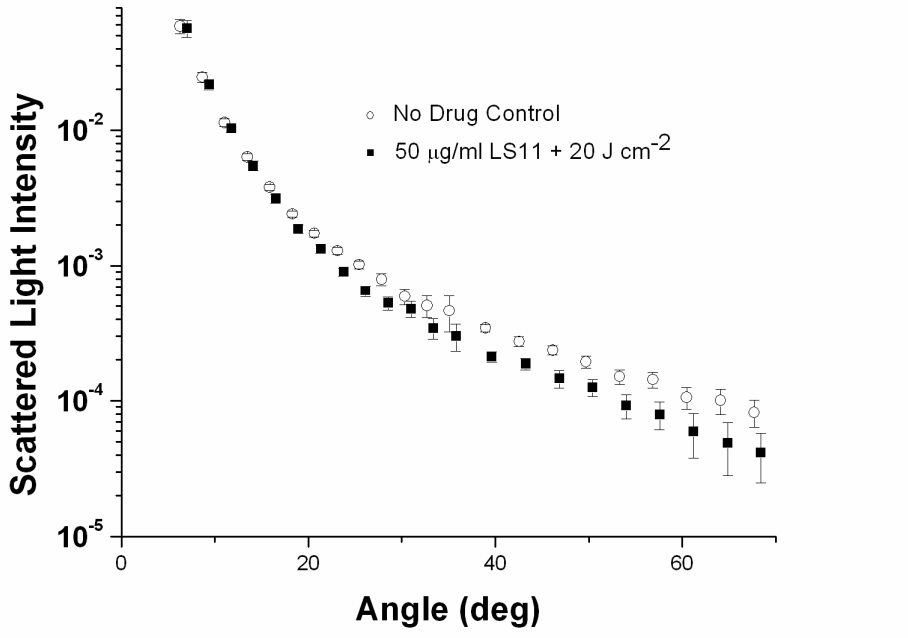

Figure 5. Scattering data from EMT6 cells subjected to 20 J cm^{-2} LS11 PDT and from no-drug control cells.

Scattering data from cells subjected to 20 J cm^{-2} of LS11 PDT and cells subjected to neither drug nor treatment are displayed in Figure 5. Contrary to previous studies involving mitochondrial damage, damage to lysosomes effects scattering at angles greater than about 15°. This is very consistent with damage to organelles smaller than mitochondria, as larger organelles are more highly forward scattering.

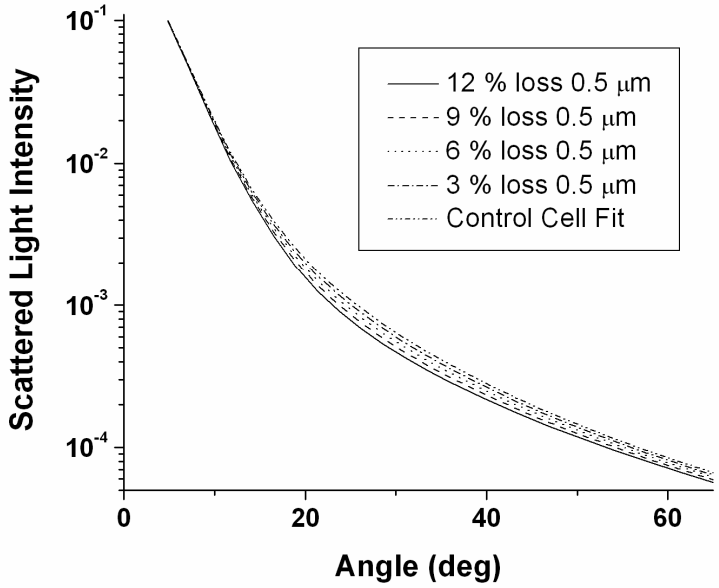

Figure 6. Forward-calculated, angularly-resolved light scattering based on reducing the amount of light scattered by a 0.5 m population.

This is demonstrated in Figure 6, which shows forward calculations based on the Mie theory fit to the control cells with the subtraction of various σρ contributions of a 0.5 m population of light scatterers. In Figure 6, the curve representing a 12% reduction in total scattered light by a candidate lysosomal population agrees best with the two data sets.

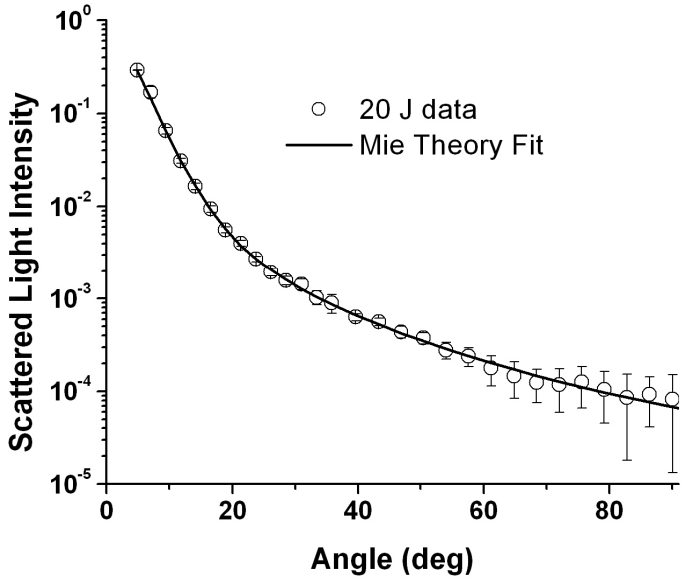

Figure 7. Scattering data and Mie theory fit to cells subjected to 20 J cm^{-2} LS11 PDT.

A Mie theory fit to the 20 J cm^{-2} LS11 PDT data is displayed in Figure 7. In this case, a homogenous sphere model was appropriate to fit the post-treatment data, whereas in the case of ALA/PPIX-treated cells a coated sphere model based on mitochondrial swelling was necessary. The analysis of these data is still in progress.

3.2.2 Scattering from LS11-incubated cells vs. no drug controls

In the previous section, we reported on the observation of scattering differences between cells subjected to an LS11 PDT dose which ablated a significant fraction of lysosomes and cells that were not loaded with LS11. In this section, we report on the observation of scattering changes between cells that were loaded with LS11 but not irradiated, and cells that were not loaded with LS11.

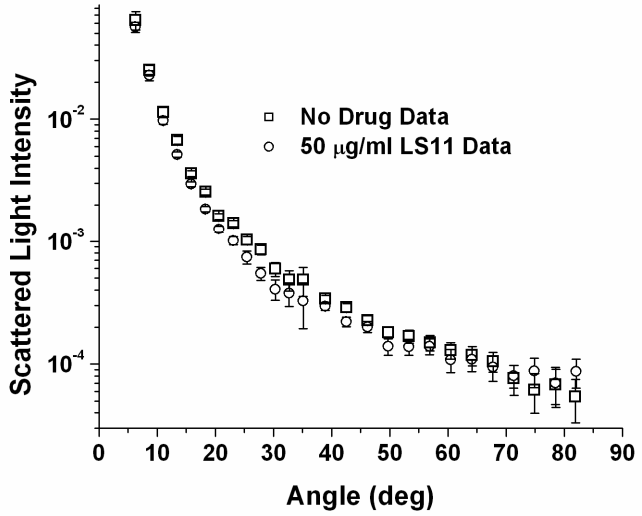

Figure 8. Scattering data from both no-drug control cells and cells incubated with LS11 but not irradiated. Scattering data were acquired at 633 nm.

Scattering data for cells loaded with 50 g/mL LS11 and those that were not loaded with drug are displayed in Figure 8. The scattering changes shown in this figure are very consistent with those for the 20 J cm^{-2} LS11 case in the angular range from ~15-40^{o} and are certainly not compatible with mitochondrial swelling, as scattering in the forward direction is nearly identical in both the no-drug control and the drug-only control cases. Both of these measurements were made using 633 nm light from a HeNe laser, where LS11 has significant extinction. We hypothesize that these scattering changes are the result of adding LS11, which has very high extinction, directly to lysosomes. As reported in Wilson and Foster[3], the scattering phase function from a collection of particles, $P(\theta)$, takes the form

$$P_{total}(\theta) = \frac{\int \sigma(r)\rho(r)P(r,\theta)dr}{\int \sigma(r)\rho(r)dr} \qquad (1)$$

where σ is the scattering cross section and ρ is the particle size distribution. It is the product $\sigma\rho$ to which these measurements are in fact sensitive. In all of our previous reports, we have used photodynamic therapy to perturb or

obliterate single organelle populations, such as mitochondria and lysosomes, to see their contribution to whole cell scattering. In those cases, we adjusted $\rho(r)$ with our photodynamic insult. In our current study, by adding extinction directly to lysosomes, we have in effect lowered the scattering cross section, $\sigma(r)$, of these lysosomes.

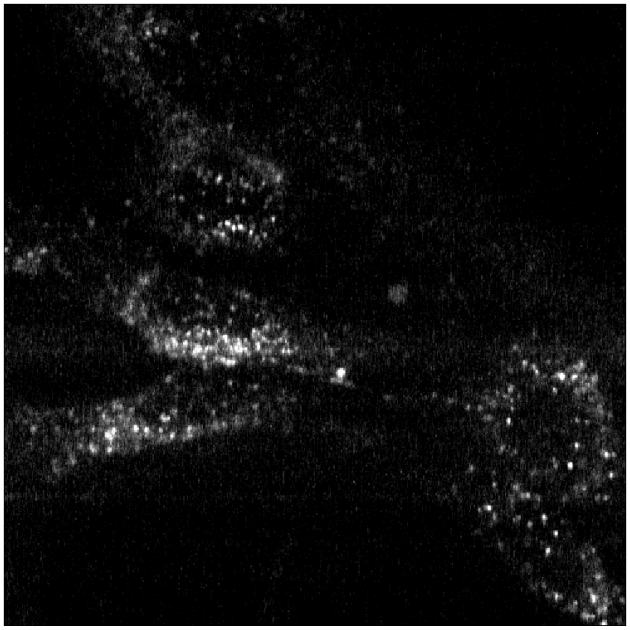

Figure 9. Confocal fluorescence image of EMT6 cells loaded with 50 g/ml LS11

The fact that the addition of LS11 to cells can affect its angularly resolved light scattering is a potentially interesting result. We have provided evidence that this phenomenon is due to adding this high-extinction photosensitizer to lysosomes, whereas photosensitizers such as ALA-induced PPIX, with their lower extinction, did not influence the scattering. An interesting comparison to make is with scattering between no-drug control cells and cells loaded with the

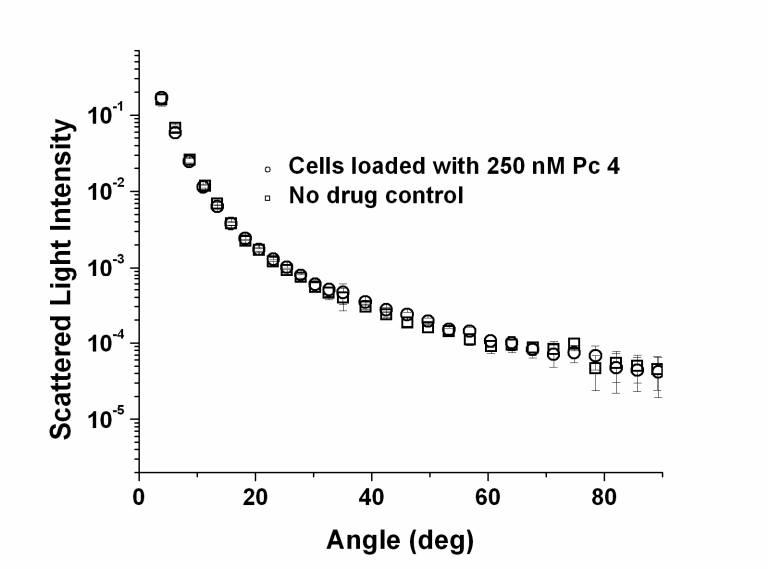

Figure 10. Angularly resolved light scattering data from both no-drug control cells and from cells incubated overnight with 250 nM Pc 4. Pc 4 is a known mitochondrial localizing photosensitizer in contrast to LS11, which localizes in lysosomes.

photosensitizer Pc 4. Pc 4 has been shown to localize to mitochondria and has a molar extinction at its absorption maximum much greater than that of LS11[7]. Shown in Figure 10 is scattering data for both no-drug control cells and for cells loaded with 250 nM Pc 4. There is no discernable difference between the two. One possible reason for scattering changes due to LS11 but not Pc 4 is the unusually strong localization of LS11 to lysosomes, as shown in Figure 9. The same affinity of Pc 4 to mitochondria is not seen in other studies[8]. The details of this discrepancy are being studied.

ACKNOWLEDGMENTS

We thank Light Sciences Corporation for making LS11 available to us for these studies. We further acknowledge Soumya Mitra for guidance with LS11 incubation and treatment conditions, and Ken Kang-Hsin Wang for help with confocal imaging. This work was supported by NIH grant CA68409.

Email addresses for J.D. Wilson and T.H. Foster are jdwilson@pas.rochester.edu and thomas.foster@rochester.edu.

REFERENCES

1. L. T. Perelman, V. Backman, M. Wallace, G. Zonios, R. Manoharan, A. Nusrat, S. Shields, M. Seiler, C. Lima, T. Hamano, I. Itzkan, J. Van Dam, J. M. Crawford, and M. S. Feld, "Observation of periodic fine structure in reflectance from biological tissue: A new technique for measuring nuclear size distribution," *Phys. Rev. Lett.,* **80**, 627-630 (1998).

2. J. D. Wilson, C. E. Bigelow, D. J. Calkins, and T. H. Foster, "Light scattering from intact cells reports oxidative-stress-induced mitochondrial swelling," *Biophys. J.* **88**, 2929-2938 (2005).

3. J. D. Wilson and T. H. Foster, "Mie theory interpretations of light scattering from intact cells," *Opt. Lett.* **30**, 2442-2444 (2005).

4. J. R. Mourant, T. M. Johnson, S. Carpenter, A. Guerra, T. Aida, and J. P. Freyer, "Polarized angular dependent spectroscopy of epithelial cells and epithelial cell nuclei to determine the size scale of scattering structures," *J. Biomed. Opt.* **7**, 378-387 (2002).

5. M. I. Mischenko, L. D. Travis, and A. A. Lacis, *Scattering, absorption, and emission of light by small particles*, (NASA Goddard Institute for Space Studies, New York, 2004).

6. J. J. Reiners, Jr., J. A. Caruso, P. Mathieu, B. Chelladurai, X. M. Yin, and D. Kessel, "Release of cytochrome c and activation of pro-caspase-9 following lysosomal photodamage involves Bid cleavage," *Cell Death Differ.* **9**, 934-944 (2002).

7. M. Lam, N. L. Oleinick, and A. L. Nieminen, "Photodynamic therapy-induced apoptosis in epidermoid carcinoma cells. Reactive oxygen species and mitochondrial inner membrane permeabilization," *J. Biol. Chem.* **276**, 47379-47386 (2001).

8. N. S. Trived, H. Wang, A. Nieminen, N. L. Oleinick, and J. A. Izatt, “Quanitative analysis of Pc 4 localization in mouse lymphoma (LY-R) cells via double-label confocal fluorescence microscopy,” *Photochem. Photobiol.* **71**, 634-639 (2000).